

## Synthesis of nanocomposite coating based on TiO<sub>2</sub>/ZnAl layer double hydroxides

V. Jovanov<sup>a</sup>✉, O. Rudic<sup>b</sup>, J. Ranogajec<sup>b</sup>, E. Fidanchevska<sup>a</sup>

a. "Ss Cyril and Methodius" University in Skopje, Faculty of Technology and Metallurgy, (Skopje, Republic of Macedonia)

b. University of Novi Sad, Faculty of Technology, (Novi Sad, Serbia)

✉vojo@tmf.ukim.edu.mk

Received 21 August 2015

Accepted 23 June 2016

Available on line 1 February 2017

**ABSTRACT:** The aim of this investigation was the synthesis of nanocomposite coatings based on Zn-Al layered double hydroxides (Zn-Al LDH) and TiO<sub>2</sub>. The Zn-Al LDH material, which acted as the catalyst support of the active TiO<sub>2</sub> component (in the content of 3 and 10 wt. %), was synthesized by a low super saturation co-precipitation method. The interaction between the Zn-Al LDH and the active TiO<sub>2</sub> component was accomplished by using vacuum evaporation prior to the mechanical activation and only by mechanical activation. The final suspension based on Zn-Al LDH and 10wt. % TiO<sub>2</sub>, impregnated only by mechanical activation, showed the optimal characteristics from the aspect of particle size distribution and XRD analysis. These properties had a positive effect on the functional properties of the coatings (photocatalytic activity and self-cleaning efficiency) after the water rinsing procedure.

**KEYWORDS:** Composite; Durability; Characterization; Microstructure; Particles size distribution

**Citation/Citar como:** Jovanov, V.; Rudic, O.; Ranogajec, J.; Fidanchevska, E. (2017) Synthesis of nanocomposite coating based on TiO<sub>2</sub>/ZnAl layer double hydroxides. *Mater. Construcc.* 67 [325], e112. <http://dx.doi.org/10.3989/mc.2017.07215>.

**RESUMEN:** *Síntesis de un revestimiento nanocompuesto basado en TiO<sub>2</sub> / ZnAl hidróxidos dobles en capas.* El objetivo de esta investigación fue la preparación de recubrimientos de nanocompuestos basados en Zn-Al hidróxidos dobles en capas (Zn-Al LDH) y TiO<sub>2</sub>. El material de LDH Zn-Al, que actuaba como catalizador del componente activo TiO<sub>2</sub> (en el contenido de 3 y 10 en peso.%), se sintetizó por un método de co-precipitación con baja sobresaturación. La interacción entre el Zn-Al LDH y el componente activo TiO<sub>2</sub> se llevó a cabo mediante el uso de la evaporación al vacío antes de la activación mecánica y sólo por activación mecánica. La suspensión final basada en Zn-Al LDH y 10wt. % TiO<sub>2</sub>, impregnada solamente por la activación mecánica, mostró las características óptimas desde el aspecto de la distribución de tamaño de partícula y análisis de XRD. Estas propiedades tenían un efecto positivo sobre las propiedades funcionales de los revestimientos (actividad fotocatalítica y eficiencia de auto-limpieza) después del procedimiento de aclarado de agua.

**ORCID ID:** V. Jovanov (<http://orcid.org/0000-0001-7734-0757>); O. Rudic (<http://orcid.org/0000-0003-0468-1432>); J. Ranogajec (<http://orcid.org/0000-0002-9831-2998>); E. Fidanchevska (<http://orcid.org/0000-0003-2919-5916>);

**PALABRAS CLAVE:** Compuesto; Durabilidad; Caracterización; Microestructura; Distribución de tamaños de partículas

**Copyright:** © 2017 CSIC. This is an open-access article distributed under the terms of the Creative Commons Attribution License (CC BY) Spain 3.0.

## 1. INTRODUCTION

Titanium-dioxide ( $\text{TiO}_2$ ) has been extensively studied recently in the field of environmental protection due to its high photocatalytic efficiency in the processes of water and air purification (1–4). Among many candidates for photocatalysts,  $\text{TiO}_2$  is almost the only material suitable for this application because it has presented the most efficient photoactivity, the highest stability, and the lowest cost and nontoxicity (5–7).

In spite of the fact that  $\text{TiO}_2$  is currently regarded as a nontoxic material, the possibility of  $\text{TiO}_2$  to be a biohazard has still remained open (8–9) due to the risk of  $\text{TiO}_2$  nanoparticles being discharged into the environment. The simplest way to solve this problem is to impregnate these particles into a suitable substrate. Associating  $\text{TiO}_2$  nanoparticles to a crystalline substrate allows their easy manipulation. Tennakone et al. (10) studied the photocatalytic activity of  $\text{TiO}_2$  supported on polythene films. It was found that  $\text{TiO}_2$  could be supported on polythene films (commercial polythene film, thickness 0.006 cm) without inhibiting its photocatalytic activity. In search of a cheap titania-immobilized photocatalyst, it was found that the coal fly ash could be a good mineral support for the  $\text{TiO}_2$  photocatalyst (11). According to Zainudin et al. (12), beyond certain level of  $\text{TiO}_2$  loading, it is important to optimize the catalyst composition in order to avoid aggregation of the  $\text{TiO}_2$  particles or their being discarded from the supporter. Xagas et al. (13) reported that the photocatalytic properties of the immobilized  $\text{TiO}_2$  film are affected by the preparation technique of the  $\text{TiO}_2$  film.

Layer double hydroxides (LDH), also known as hydrotalcite, – present the largest group of materials which can be synthetically produced by using different methods such as sol gel, hydrothermal precipitation (14) or co-precipitation. Among various types of hydrotalcite, the Zn/Al LDH has been broadly synthesized in the recent years because of its favorable textural, acid-base and redox properties. These properties can be successfully tailored during synthesis because parameters such as pH value,  $\text{Zn}^{2+}/\text{Al}^{3+}$  molar ratio and temperature of calcination significantly affect the characteristics of the synthesized powder (particle size distribution, specific surface area, photoactivity, etc. (15,16). Seftel et. al (15) synthesized Zn/Al LDHs with cationic ratio of 1-4 by the conventional co-precipitation method at pH=7.5. The largest amounts of ZnO were formed after the thermal treatment at  $T=500^\circ\text{C}$  influencing the photocatalytic activity of the final product. Namely, the Zn/Al LDH with cationic ratio 4 can remove 93% of the methyl-orange dye (15). The synthesized Zn/Al LDH with a  $\text{Zn}^{2+}/\text{Al}^{3+}$  molar ratio of 1.48 photodegraded phenol and p-cresol up to 95% after 4 and 6 hours

of irradiation, respectively. The synthesized Zn/Al LDH showed better degradation of organic pollutant compounds in comparison to  $\text{TiO}_2$  (16).

The Zn/Al LDH materials have been receiving increasingly more attention as the supports of the  $\text{TiO}_2$  particles forming LDH/ $\text{TiO}_2$  nanocomposites. The  $\text{TiO}_2$  nanoparticles associated with the LDH substrate retain their photoactivity and do not endanger either the environment or human health. Moreover, the  $\text{TiO}_2$  nanoparticles are embedded in the structure of a porous LDH avoiding the formation of macroscopic aggregates that may lead to the diminution of their efficiency. Furthermore, LDHs are stable supports that protect the  $\text{TiO}_2$  particles from washing or erosion; they are non-toxic and present inexpensive materials (17–20).

The main purpose of the present study was the synthesis and characterization of  $\text{TiO}_2/\text{ZnAl-LDH}$  active nanocomposites and suspensions. For that purpose, first LDH was synthesized and then the small sized  $\text{TiO}_2$  particles were embedded into the structure of the LDH by using two different methods of impregnation: vacuum evaporation impregnation prior to mechanical activation and impregnation only by mechanical activation. The synthesized coatings were characterized from physical, mineralogical and morphological aspect. The decomposition efficiency of Rhodamine B was chosen as the test reaction for the investigation of photocatalytic activity of the synthesized powders and suspensions. Also, the functional properties (photoactivity and self-cleaning efficiency expressed through the contact angle measurements) were determined before and after the water rinsing procedure in order the durability of the nanocomposites to be characterized for.

## 2. MATERIALS AND METHODS

### 2.1. Material and sample preparation

The Zn-Al LDHs were synthesized by a low super saturation co-precipitation method at constant pH value (9–9.5). The synthesis was realized at constant temperature ( $40^\circ\text{C}$ ) by intensive stirring. The chosen precursors  $\text{Zn}(\text{NO}_3)_2 \cdot 6\text{H}_2\text{O}$  and  $\text{Al}(\text{NO}_3)_3 \cdot 9\text{H}_2\text{O}$  with molar ratio of 0.7 M and 0.3 M, respectively, were continuously added ( $4 \text{ cm}^3/\text{min}$ ). For pH regulation, alkali solution of the  $\text{Na}_2\text{CO}_3$  and  $\text{NaOH}$  with a concentration of 0.67 M and 2.25 M, respectively, were employed. The obtained precipitate was aged at  $40^\circ\text{C}/24\text{h}$  by constant stirring at 200 rpm, washed with demineralized water until pH 7, and then dried at  $100^\circ\text{C}/24\text{h}$  prior to the calcination at  $500^\circ\text{C}/24$  (21).

The active ZnAl-LDH/ $\text{TiO}_2$  nanocomposite powder was obtained by the impregnation

of TiO<sub>2</sub> suspension (in contents of 3 and 10 wt. %) into Zn-Al-LDH calcined powder. The commercial TiO<sub>2</sub> suspension (80 wt.% anatase and 20 wt.% rutile; grain size < 100 nm; content of dry matter 30.0 ± 1.0 wt. % and pH 7), used for this purpose, was obtained from Degussa company, Germany. The process of impregnation was carried out in an alkali solution (pH= 9–9.5) by vacuum evaporation, prior to the mechanical activation (the first protocol), and only by mechanical activation (the second protocol). The pH value during impregnation was maintained with the same basic solutions (0.67 M Na<sub>2</sub>CO<sub>3</sub> and 2.25 M NaOH) as in the previous process of Zn-Al-LDH synthesizing.

The impregnation by vacuum evaporation was realized in a rotary vacuum evaporator (DEVAROT) at 55°C for 30 min. Further on, the obtained powder was mechanically activated in a planetary mill during 180 min using the speed of 200 rpm, while the material and ball ratio was 1:5. The process of impregnation performed only by mechanical activation was realized in an attritor mill for 90 min with the speed of 1500 rpm, in air atmosphere (material: ball ratio was 1: 5).

According to the way of impregnation and the TiO<sub>2</sub> content, the obtained ZnAl-LDH/TiO<sub>2</sub> nanocomposite powders were assigned as: A1 and A2 representing ZnAl-LDH/TiO<sub>2</sub> nanocomposite powders with 3 and 10wt.% TiO<sub>2</sub> content, respectively, impregnated by vacuum evaporation prior to mechanical activation and B1 and B2 representing ZnAl-LDH/TiO<sub>2</sub> nanocomposite powders with 3 and 10wt.% TiO<sub>2</sub> content, respectively, impregnated only by mechanical activation.

The nanocomposite suspension was formed by suspending ZnAl-LDH/TiO<sub>2</sub> powder (in a quantity of 0.1 and 0.5g) into demineralized water (100 ml) by using di-ammonia-hydrogen citrate as a dispersing agent and by a stirring procedure at 300 rpm, for 1hour. Ultrasonic bath was used for 30 min in order to prevent possible agglomeration.

The obtained nanocomposite suspension was applied onto the surface of clay roofing tile samples by using spray technique in the following conditions: spraying pressure was 6.5 MPa, distance of the spray device from the sample was 90 cm, angle of spraying was 45°, and diameter of nozzle was 1.3 mm. The coated roofing tile samples were afterwards dried at RT/24h.

## 2.2. Characterization

The particle size distribution of the synthesized ZnAl-LDH/TiO<sub>2</sub> nanocomposite powder was determined by Malvern Instruments, zeta-nanoseries, NanoZS under the following conditions: refraction index of the investigated suspensions ( $n = 1.55$ ), light absorption ( $a = 0.3$ ) and pH value = 9.

The X-ray diffraction (XRD) was performed by Philips PW 1710 device in order to determine the phase composition of the designed nanocomposite powders. The employed conditions for this investigation were: monochromatic CuK $\alpha$  radiation with  $\lambda = 1.5418 \text{ \AA}$  in the 5–55° of 2° range, scan rate 0.02°, 0.5 s per step.

The photocatalytic activity of the obtained nanocomposite powders was determined spectrophotometrically by monitoring the photocatalytic degradation of Rhodamine B (RhB) used as a model pollutant in the photocatalytic tests. The photocatalytic tests were performed on the newly synthesized ZnAl-LDH/TiO<sub>2</sub> powders and ZnAl-LDH/TiO<sub>2</sub> suspensions. The suspension was sprayed onto the samples (4x4x1 cm) of clay roofing tiles (total porosity: 32.93% roughness evaluated by R<sub>a</sub>: cca 3  $\mu$  m). The powder and the coated clay roofing tile samples were UV/VIS irradiated (EVERSUN lamp, intensity of UV-A and Visible light spectra were 0.8 mWcm<sup>-2</sup> and 0.3 Wcm<sup>-2</sup>, respectively). The distance between the UV/VIS lamp and the samples was 35 cm (20).

The photocatalytic activity tests of the powders were performed in a Pyrex flasks patch-type reactor (21). Namely, the quantity of 50 mg of the calcined ZnAl-LDH/TiO<sub>2</sub> powder was added to 100 ml RhB water solution, 10 ppm dm<sup>-3</sup>. The obtained solution was stirred for 30 min in the dark, in order to reach adsorption/desorption equilibrium between the dye and the surface of the catalysts. Aliquots of the obtained suspension were taken at definite time intervals of UV/VIS irradiation and centrifuged in order to obtain a clear solution for the analysis of the RhB content. In order to eliminate possible additional adsorption phenomena, the control solution was kept in the dark for the same reaction periods as for the UV/VIS irradiated samples. The RhB solution was used, as a blind sample, in the same UV/VIS irradiation conditions in order to confirm it's slightly photocatalytic degradation (22). All reactions were carried out at atmospheric pressure and at room temperature. The RhB concentration was measured by monitoring the major absorption peak at  $\lambda = 554 \text{ nm}$  by using UV-VIS spectrophotometer (EVOLUTION 600 spectrophotometer). The photocatalytic activity was estimated based on the efficiency of the RhB degradation, A (%). It was calculated according to the relation [1]:

$$A (\%) = [(C_0 - C)/C_0] \cdot 100 \quad [1]$$

Where:

C<sub>0</sub> is the RhB concentration of the sample in the dark at the defined time

C is the RhB concentration of sample under the UV light irradiation at defined time.

In order to enable direct contact between the active surface of the clay tile sample and the dye/

RhB solution, a glass tube ( $d = 3$  cm,  $h = 6$  cm) was fixed with silicon on the surface of each tile sample and filled with 12 ml of the dye/RhB solution. Considering that the porosity and roughness of the substrate (clay roofing tiles) is an important parameter that may control photocatalytic activity, a pre-absorption test of RhB solution was also carried out in order to saturate samples before the photocatalytic test. It was possible to change the color of RhB solution during the examination of photocatalytic activity even without any photocatalytic coating, due to the occurrence of RhB absorption by the substrate. Namely, the tile samples were submerged (24h) in a glass tank filled with the RhB solution with the same concentration ( $10 \text{ ppm dm}^{-3}$ ). During the pre-absorption test, the solution of RhB in the glass tubes and in the tank was constantly replaced with a fresh solution until the tiles were saturated and the difference in color concentration between the two consecutive measurements was within the limit of 5%. After the pre-absorption period, the RhB solution was replaced with a new one freshly prepared. At defined time intervals of UV/VIS irradiation and correspondingly the samples kept in the dark, aliquots of glass tube solution were taken for spectrophotometric concentration testing.

The photocatalytic activity of the coatings was estimated by degradation efficiency of the RhB solution by using the same formula as for the powder samples (18).

The contact angle between the appropriate experimental fluid (glycerol) and the surfaces of the coated samples, before and after water rinsing procedure, was measured by using Surface Energy Evaluation System, Advex Instruments, (Brno, Czech Republic). The liquid droplets of about 5  $\mu\text{l}$  in volume were gently deposited on the coated substrate using a micro syringe. All measurements of the initial contact angle ( $\theta_{ci}$ , after 1 s) at room temperature were performed at five different points for each of three specimens of the investigated samples. Each droplet deposited onto surface was measured five times.

Water rinsing durability test was performed in order to define the stability of the coating in the severe conditions (rain rinsing procedure) on the porous clay tile. The rinsing procedure was simulated in laboratory conditions by using the equipment which provides constant tap water flow (0.04 l/s) through a pipe system (nozzle diameter of 0.90) and water fall (height of 50 cm) on the sample (set at an angle of  $45^\circ$ ). The duration of the test was 30 min.

The functional properties (photocatalytic activity and self-cleaning efficiency) of the coated tiles were measured before and after the rinsing procedure during UV/VIS irradiation. The RhB (10ppm) was used as the model pollutant for photocatalytic

activity assessment while the contact angle measurements for the estimation of self-cleaning properties.

### 3. RESULTS AND DISCUSSION

#### 3.1. Particle size distribution of the impregnated ZnAl-LDH/TiO<sub>2</sub> powders

Particle size distribution of the ZnAl-LDH/TiO<sub>2</sub> powders impregnated by vacuum evaporation and then mechanically activated (A1 and A2) and only mechanically activated (B1 and B2) are presented in Figure 1.

The diagram presented in Figure 1, shows that the powders impregnated by vacuum evaporation and then mechanically activated have significantly larger particle size distribution compared with the powders impregnated only by mechanical activation. The sample A2 has a bimodal particle size distribution and mostly contains particles with diameters of 1718 nm and 5560 nm. On the other hand, for the powder A1 a three-modal particle size distribution is evident i.e. they are mainly distributed in three intervals with the maximum particle diameters: 825 nm, 1718 nm and 5560 nm. As opposed to the A1 and A2 powders, which possess a wide range of particle size distribution mainly in micrometric range, the powders B1 and B2 have a finer and mono-modal particle size distribution. Namely, the B2 powder contains particles with diameters from 10 to 1700 nm. The registered diameter maximum is 459 nm. As for the sample B2, the powders B1 have a relative mono-modal particle size distribution, but it is also evident that only a small quantity of the particles are in the interval between 3000 and 6000 nm. This system

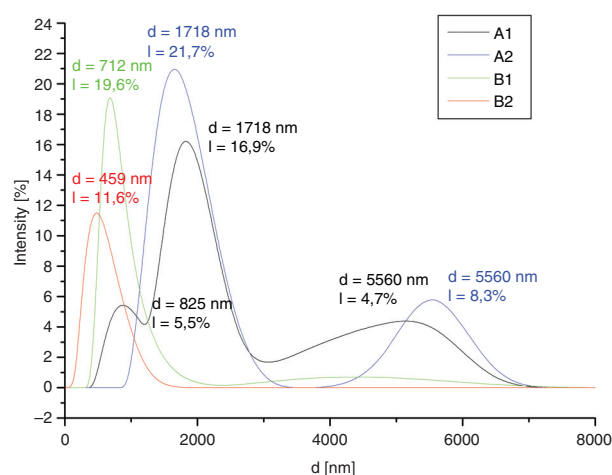


FIGURE 1. Particle size distribution of the ZnAl-LDH/TiO<sub>2</sub> powders impregnated by vacuum evaporation prior to the mechanical activation (A1 – 3wt.% TiO<sub>2</sub>, A2 – 10wt.% TiO<sub>2</sub>) and only mechanically activated (B1 – 3wt.% TiO<sub>2</sub>, B2 – 10wt.% TiO<sub>2</sub>).

contains 19.6 % of particles with the diameter of 712 nm.

### 3.2. Phase composition of the impregnated ZnAl-LDH/TiO<sub>2</sub>

The X-ray diffractograms of the obtained powders are shown in Figure 2.

Generally, regarding the procedure of the TiO<sub>2</sub> impregnation, differences in the intensity of the identified peaks can be observed from the XRD diffractograms. This indicates that there are differences in the phase composition (presence and step of crystallinity) of the analyzed powders. Namely, the powders impregnated only by mechanical activation (powders B1 and B2) show significantly higher crystallinity compared to the powders impregnated in a vacuum evaporator prior to the mechanical activation (A1 and A2). The XRD measurements of the samples also revealed that the crystallinity of the samples depends not only on the amount of the impregnated TiO<sub>2</sub>, but also on the procedure of impregnation.

As for the sample of B1 (3wt.% TiO<sub>2</sub>), it can be noticed that LDH (JCPDS 38-0486) and ZnO

(JCPDS 80-0075) are the only dominant phases. Evidently, the TiO<sub>2</sub>, anatase crystal phase (JCPDS 84-1286), was dispersed in the intermediate LDH layers. It is an interesting fact that LDH appears mainly as the dominant phase although this carrier of the photocatalytic active component TiO<sub>2</sub> was calcinated before the impregnation process. This phenomenon points towards the conclusion that in this sample the memory effect was achieved. Namely, returning of the structure of the mixed oxides into the memory of the original structure of the layered double hydroxides during the process of impregnation was present (23). For the sample B2 (10wt.% TiO<sub>2</sub>), the reflections of the LDH possess higher intensity indicating a higher memory effect and return to the layered double structure in comparison with the powder B1. It can be concluded that the increase in the quantity of the impregnated TiO<sub>2</sub> to 10wt.% does not inhibit the memory effect of the calcinated active carrier. On the contrary, it has a positive effect on the crystallinity and on stability of the ZnO and Zn<sub>2</sub>TiO<sub>4</sub>, which is important for the upcoming photocatalytic reactions (24). The lower crystallinity of the TiO<sub>2</sub>, ZnO and Zn<sub>2</sub>TiO<sub>4</sub> in the case of the powders A1 and A2 could be responsible for their lower photocatalytic activity.

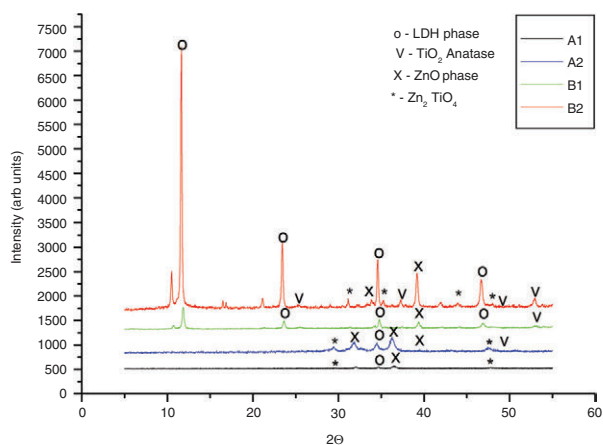


FIGURE 2. X-ray diffractograms of the powders A1, A2, B1 and B2.

### 3.3. Morphology

Figure 3 shows the morphological changes of the ZnAl-LDH/TiO<sub>2</sub> powders along with the increase of the TiO<sub>2</sub> content of the mono modal powder samples, B1 and B2. In the case of both powders, it is evident that the typical morphology for the LDHs, agglomerates of the flat particles named “desert rose”, were identified (24–26). The spherical TiO<sub>2</sub> particles in the form of agglomerates most frequently preferably appear on the LDH particles’ edges (27) of the “desert rose”.

This observation implies the idea that the rigid, smooth plain surface of the LDH particles without cracks are not a suitable matrix for the TiO<sub>2</sub> incorporation (24–26). Generally, it was found

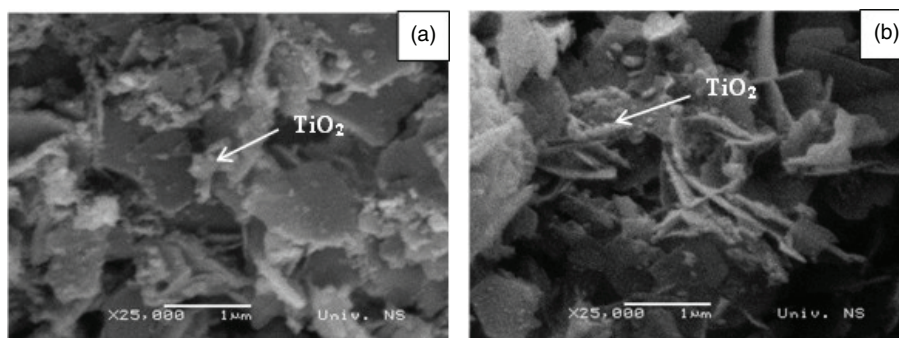


FIGURE 3. SEM micrographs of ZnAl-LDH/TiO<sub>2</sub> powders obtained only by mechanical activation (a. B1 - 3wt.% TiO<sub>2</sub>, b. B2 - 10wt.% TiO<sub>2</sub>).

that a slight increase of TiO<sub>2</sub> spherical particles is in direct correlation to the greater amount of TiO<sub>2</sub> previously impregnated into the LDH structure. No remarkable change of the surface morphology was observed in either one of the analyzed systems.

The presence of TiO<sub>2</sub> on the LDH particles edges was additionally confirmed by EDS (Energy Dispersive Spectroscopy) analysis (Table 1) of the samples, Figure 4.

The results of the EDS analysis (Table 1) in the spectra of the both samples, beside the Ti presence, detected the existence of the basic building metals, zinc and aluminum, of the LDH form. Successful impregnation of the TiO<sub>2</sub> into the LDH carrier was confirmed.

### 3.4. Photocatalytic activity testing of the impregnated LDH with TiO<sub>2</sub>

The results from the testing of the photocatalytic activity during a period of 24h irradiation with UV/VIS rays (powder systems A1, A2, B1 and B2 and blank sample of RhB solution) are shown in the Figure 5.

As shown in Figure 5, the RhB was degraded ~3% under the UV/VIS irradiation without the presence of the catalyst (blank sample), indicating that photolysis reaction also contributes to a slightly degradation of the dye. However, even by taking this effect into account, the photo-degradation of RhB was enhanced remarkably in the presence of the above mentioned synthesized photocatalysts. Also, it was evident that after 210 min (3.5h) of UV/VIS radiation, the highest photoactivity value for the sample B2 was 90.87% while

for sample B1 it was only 32%. Samples A1 and A2, after this time of irradiation, possessed almost the same photoactivity values i.e. only 18%. By increasing the time of UV/VIS irradiation up to 1440 min (24 h) it was evident that samples B2 and B1 reached almost the maximal value of the photoactivity. The photoactivity of the samples B1 and A2 also increased up to 94,06% and 61,45%, respectively, but there was no changes of the photocatalytic activity of the powder A1. Generally, it can be concluded, from Figure 5, that the powders impregnated only by mechanical activation (B1 and B2) and the samples impregnated with 10 wt.% TiO<sub>2</sub> (B2 and A2) showed better photocatalytic activity. In addition, higher photocatalytic activity of B1 and B2 samples can be attributed to their finer particle size distribution (Figure 1) that could offer a higher surface for the RhB adsorption than A1 and A2 samples. Also, higher crystallinity of B1 and B2 samples enabled higher RhB degradation. In general, the way of TiO<sub>2</sub> impregnation, either by mechanical activation or by vacuum evaporation prior to the mechanical activation has the crucial impact on the photocatalytic activity. The former way of impregnation is preferable for reaching better photocatalytic activity.

Based on the obtained results of the photocatalytic activity, the powders B2 and A2 from groups A and B, were further used for the creation of photocatalytic suspensions which were later deposited by spray technique on the surface of the clay roofing tile samples used as porous substrates, Figure 6.

The values of the photocatalytic activities of the coating composed of 0.1g B2 powder, after UV/VIS irradiation of 210 min (3.5 h) and 1440 min (24 h),

TABLE 1. EDS analysis for the samples B1 and B2

	C	O	Al	Ti	Zn	Total
B1 spectrum 1	19.56	37.5	7.45	2.3	33.18	100
B2 spectrum 1	23.06	34.75	5.62	4.45	32.13	100

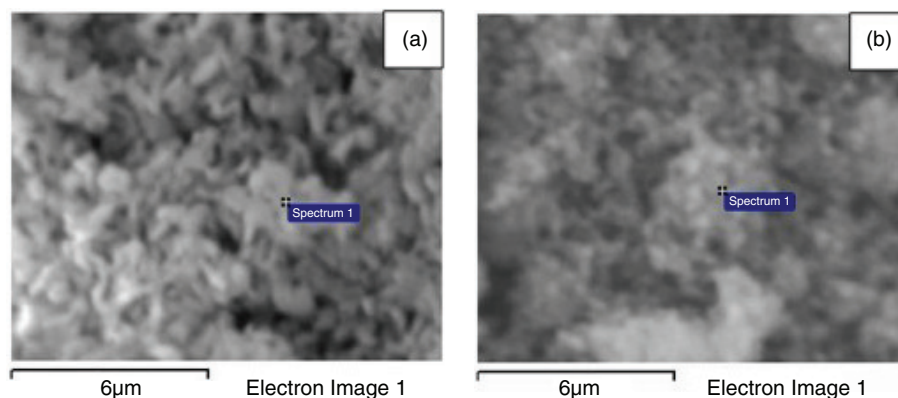


FIGURE 4. SEM micrographs of the location of EDS spectra in the samples B1 (a) and B2 (b).

are 7.61% and 22.28%, respectively, while the coating composed of 0.1g A2 powder, showed insignificant values of the photocatalytic activity even after (24 h) of UV/VIS irradiation.

Based on the results above, a new suspension with 0.5g of the powder B2 was prepared in the same conditions as in the case of the previously two B suspensions and deposited onto the ceramic samples (porous substrate). The results from Figure 6 show an increase of the photocatalytic activity up to 17.57 % after 3.5 h of UV/VIS irradiation and 62.16% after 24 h of UV/VIS irradiation for the suspension with 0.5g of the powder B2. Comparing these results with the activities of the coating containing only 0.1 g of the powder system B2, Figure 6, it can be concluded that the catalyst carrying 0.5g B2 significantly affected the increase of the photocatalytic activity of the LDH/TiO<sub>2</sub> coating. This system was further the object of the water rinsing investigation.

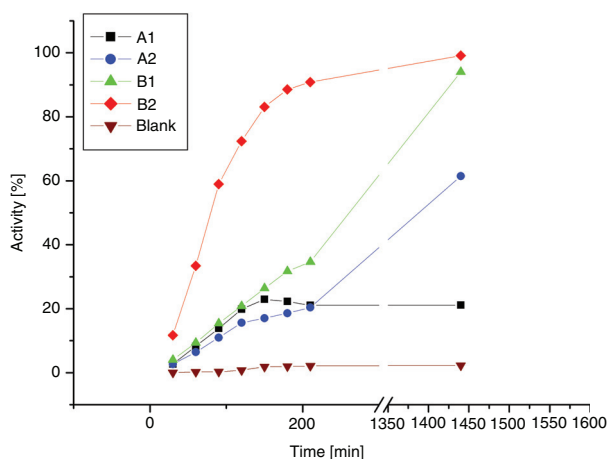


FIGURE 5. Photocatalytic activity of A1, A2, B1 and B2 powder samples and of the blank sample of RhB solution.

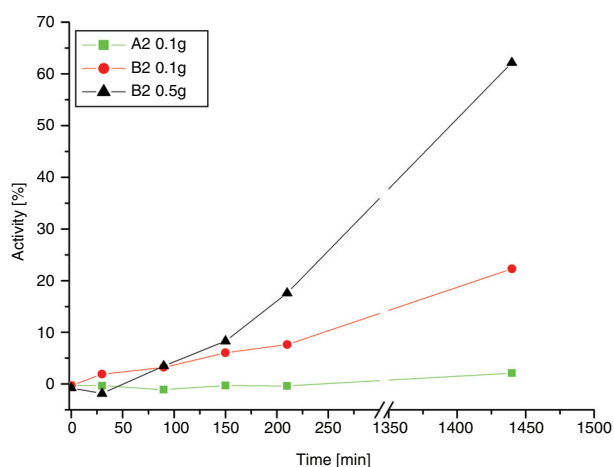


FIGURE 6. Photocatalytic activity of the coatings formed with 0.1g A2 /B2 powder and 0.5g B2 powder.

### 3.5. Water rinsing durability of the coating

The water rinsing durability of the coating with the best photocatalytic activity (B2 with 0.5g of the powder) was investigated regarding the two main functional properties: photocatalytic activity and self-cleaning efficiency. The clay tiles coating formed with 0.5g of the B2 suspension were previously exposed to water rinsing procedure (30 min) and then the photocatalytic activity and self-cleaning efficiency were analyzed. The obtained results are presented in Figures 7 and 8.

The results of the photocatalytic activity after rinsing procedure showed a small decline in terms of the measurements made before the rinsing procedure, Figure 7. During irrigation, the poorly bound TiO<sub>2</sub> particles were removed. Namely, the values of the photocatalytic activity after rinsing procedure was 10.09% (210 min) of UV/VIS irradiation, and 54.26% after 1440 min of irradiation, while before rinsing procedure, these values had been slightly higher (17.57 % after 210 min of UV/VIS irradiation and 62.16% after 1440 min of UV/VIS irradiation). The noticed difference indicates a good stability of the synthesized coating B2 to rinsing procedure which is a significant characteristic regarding its application.

The assessment of the self-cleaning properties of the coated substrate was performed by the measurements of the initial contact angle,  $\theta_{ci}$  (Figure 8). The decreasing of the both  $\theta_{ci}$  values, before and after water rinsing procedure, with UV/VIS irradiation, directly confirms the presence of the strong self-cleaning effect. Generally, the values of the contact angle (lower than 90°) proved the existing of hydrophilicity of the coating before and after water rinsing procedure which is of great importance for self-cleaning behavior.

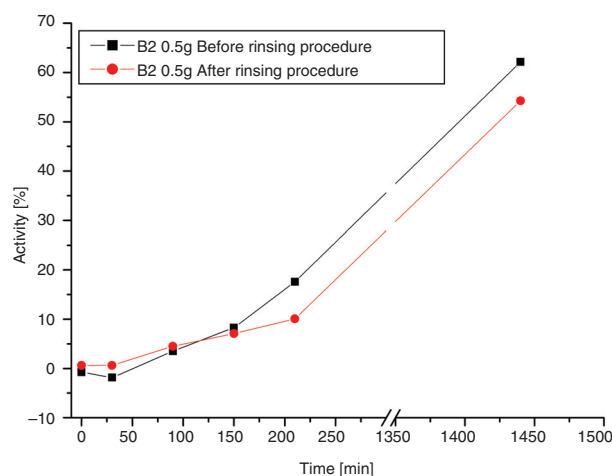


FIGURE 7. Photocatalytic activity of the coating formed with 0.5g B2 powder, before and after the water rinsing procedure.

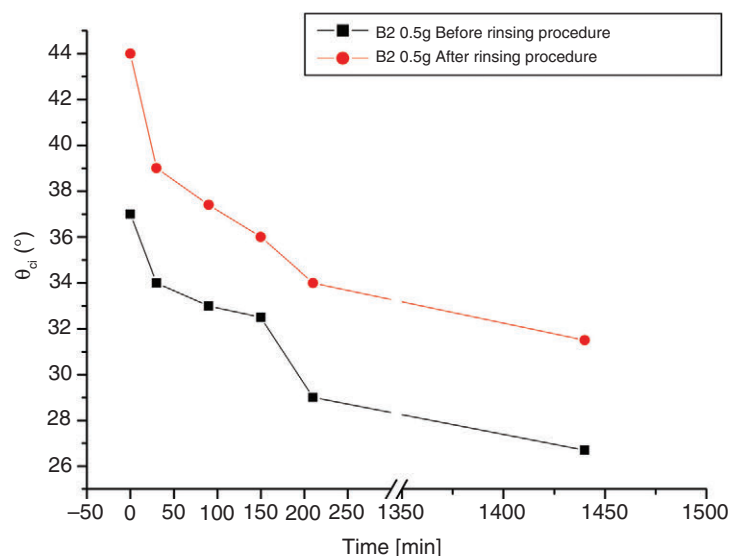


FIGURE 8. Self-cleaning efficiency assessment of the coating, formed with 0.5g B2 powder, before and after rinsing procedure

The noted differences of the  $\theta_{ci}$  values before and after water rinsing procedure were the result of a slight physical removal of the deposited ZnAl-LDH/TiO<sub>2</sub> coating. This presents some insignificant negative influence of rinsing procedure on the self-cleaning efficiency, since the same trend of the  $\theta_{ci}$  value, in both cases of the experiment, was identified. The existing decreasing trend of the  $\theta_{ci}$  values after water rinsing procedure proves a good durability and a significant compatibility of the synthesized B2 coating with the substrate of clay roofing tiles.

#### 4. CONCLUSIONS

Based on the comparative investigation of particle size distribution and XRD analysis of the designed nano-composite ZnAl-LDH/TiO<sub>2</sub> powders, it was concluded that the samples impregnated with TiO<sub>2</sub> by vacuum evaporation prior to the mechanical activation, possessed a three modal particle size distribution and smaller crystallinity, whereas the samples impregnated only by mechanical activation were characterized with a fine mono-modal particle sized distribution and a significantly higher level of crystallinity. These results indicate a strong influence of the way of TiO<sub>2</sub> impregnation on the photocatalytic powder activity.

The amount of the impregnated TiO<sub>2</sub> affected the photocatalytic activity of the obtained powders. An optimal loading of 0.5 g powder catalyst/100ml suspension of ZnAl-LDH/TiO<sub>2</sub> was found to be the most appropriate. The value of the photocatalytic activity was found to be 17.57 % after 3.5h of radiation and 62.16 % after 24h radiation. This coating shows significant durability to water rinsing, indicating a good adhesion with the surface of the porous clay roofing tile.

Based on the obtained results, the newly synthesized coating composed of ZnAl-LDH/TiO<sub>2</sub> presents a potential material that may find its use as a protective coating for inorganic porous substrates.

#### ACKNOWLEDGEMENTS

The financial support from Serbian Ministry of Education, Science and Technological Development (Contract No. III45008) is gratefully acknowledged.

#### REFERENCES

- Dai, K.; Chen, H.; Peng, T.; Ke, D.; Yi, H. (2007) Photocatalytic degradation of methyl orange in aqueous suspension of mesoporous titania nanoparticles. *Chemosphere* 69 [9], 1361–1367. <http://dx.doi.org/10.1016/j.chemosphere.2007.05.021>.
- Zhang, W.; Zou, L.; Wang, L. (2009) Photocatalytic TiO<sub>2</sub>/adsorbent nanocomposites prepared via wet chemical impregnation for wastewater treatment: A review. *Appl. Catal. A General* 371 [1–2], 1–9. <http://dx.doi.org/10.1016/j.apcata.2009.09.038>.
- Ramirez, A.M.; Demeestere, K.; De Belie, N.; Mantyla, T.; Levanen, E. (2010) Titanium dioxide coated cementitious materials for air purifying purposes: preparation, characterization and toluene removal potential. *Bulld. Environ.* 45 [4], 832–838. <http://dx.doi.org/10.1016/j.builenv.2009.09.003>.
- Sugali, H.N.; Kakati, B.K.; Verema, A. (2009) Accelerated solar photocatalytic degradation of phenol using titanium dioxide. *J. Environ. Res. Develop.* 3 [3] 763–771.
- Jiang, W.; Mashayekhi, H.; Xing, B. (2009) Bacterial toxicity comparison between nano- and micro-scaled oxide particles. *Environ. Pollut.* 157 [5], 1619–1625. <http://dx.doi.org/10.1016/j.envpol.2008.12.025>.
- Yahiro, H.; Miyamoto, T.; Watanabe, N.; Yamaura, H. (2007) Photocatalytic partial oxidation of  $\alpha$ -methylstyrene over TiO<sub>2</sub> supported on zeolites. *Catal Today.* 120 [2], 158–162. <http://dx.doi.org/10.1016/j.cattod.2006.07.039>.
- Kasibi, M.; Zemzemi, A.; Rachid, B. (2003) Photocatalytic degradation of substituted phenols over UV irradiated TiO<sub>2</sub>. *J. Photochem. Photobiol. A: Chem.*, 159 [1], 61–70. [http://dx.doi.org/10.1016/S1010-6030\(03\)00114-X](http://dx.doi.org/10.1016/S1010-6030(03)00114-X).

8. Kaegi, R.; Ulrich, A.; Sinnet, B.; Vonbank, R.; Wichser, A.; Zuleeg, S.; Simmler H.; Brunner, S.; Vonmont, H.; Burkhardt, M.; Boller, M. (2008) Synthetic TiO<sub>2</sub> nanoparticles emission from exterior facades into the aquatic environment. *Environ. Pollut.* 156 [2], 233–239. <http://dx.doi.org/10.1016/j.envpol.2008.08.004>.
9. Reijnders, L. (2009) The release of the TiO<sub>2</sub> and SiO<sub>2</sub> nanoparticles from nanocomposites. *Polym. Degrad. Stab.* 94, 873–876. <http://dx.doi.org/10.1016/j.polymdegradstab.2009.02.005>.
10. Tennakone, K.; Tilakratne, C.T.K.; Kottagoda, I.R.M. (1995) Photocatalytic degradation of organic contaminants in water with TiO<sub>2</sub> supported on polythene films. *J. Photochem. Photobio. A: Chem.* 87 [2], 177–179. [http://dx.doi.org/10.1016/1010-6030\(94\)03980-9](http://dx.doi.org/10.1016/1010-6030(94)03980-9).
11. Yu, Y. (2004) Preparation of nanocrystalline TiO<sub>2</sub>-coated coal fly ash and effect of iron oxides in coal fly ash on photocatalytic activity. *Powder. Technol.* 146 [1–2], 154–159. <http://dx.doi.org/10.1016/j.powtec.2004.06.006>.
12. Zainudin, N.F.; Abdullah, A.Z.; Mohamed, A. R. (2008) Development of supported TiO<sub>2</sub> photocatalyst based adsorbent for photocatalytic degradation of phenol, in Proceedings of the International Conference on Environment (ICENV '08), Penang, Malaysia.
13. Xagas, A.P.; Androulaki, E.; Hisika, A.; Falaras, P. (1999) Preparation, fractal surface morphology and photocatalytic properties of TiO<sub>2</sub> films. *Thin Solid Films* 357 [2], 173–178. [http://dx.doi.org/10.1016/S0040-6090\(99\)00561-1](http://dx.doi.org/10.1016/S0040-6090(99)00561-1).
14. Chrubar, N.; Gerda, V.; Megantari, O.; Misucik, M.; Omastova, M.; Heister, K.; Man, P.; Fraissard, J. (2013) Applications versus properties of Mg–Al layered double hydroxides provided by their syntheses methods: Alkoxide and alkoxide-free sol–gel syntheses and hydrothermal precipitation, *Chem. Eng. J.* 234, 284–299. <http://dx.doi.org/10.1016/j.cej.2013.08.097>.
15. Seftel, E.M.; Popovici, E.; Mertnes, M.; De Witte, K.; Van Tendeloo, G.; Cool, P.; Vansant, E.F. (2008) Zn–Al layered doublehydroxides: synthesis, characterization and photocatalytic application, *Micropor. Mesopor. Mat.* 113 [1–3], 296–304. <http://dx.doi.org/10.1016/j.micromeso.2007.11.029>.
16. Tzompantzi, F.; Mantilla, A.; Bañuelos, F.; Fernández, J.L.; Gómez, R. (2011) Improved photocatalytic degradation of phenolic compounds with ZnAl mixed oxides obtained from LDH materials, *Top. Catal.* 54 [1–4], 257–263. <http://dx.doi.org/10.1007/s11244-011-9656-3>.
17. Vulic, T.; Rudic, O.; Vucetic, S.; Lazar, D.; Ranogajec, J. (2015) Photocatalytic activity and stability of TiO<sub>2</sub>/ZnAl layered double hydroxide based coatings on mortar substrates, *Cement Concrete Comp.* 58, 50–58. <http://dx.doi.org/10.1016/j.cemconcomp.2014.12.015>.
18. Rudic, O.; Ranogajec, J.; Vulic, T.; Vucetic, S.; Cjepa, D.; Lazar, D. (2014) Photo-induced properties of TiO<sub>2</sub>/ZnAl layered double hydroxide coating onto porous mineral substrates, *Ceram. Int.* 40 [7] Part A, 9445–9455. <http://dx.doi.org/10.1016/j.ceramint.2014.02.017>.
19. Vulic, T.; Hadnadjev-Kostic, M.; Rudic, O.; Radeka, M.; Marinkovic-Neducin, R.; Ranogajec, J. (2013) Improvement of cement-based mortars by application of photocatalytic active Ti–Zn–Al nanocomposites, *Cement Concrete Comp.* 36, 121–127. <http://dx.doi.org/10.1016/j.cemconcomp.2012.07.005>.
20. Ranogajec, J.; Radeka, M. (2013) Self-cleaning surface of clay roofing tiles, in: W.A.Daoud (Ed.), *Self-Cleaning Materials and Surfaces: A Nanotechnology Approach*, Wiley-VCHVerlan 35 GmbH, Weinheim pp. 89–128.
21. Vulic, T. (2008) Clays as catalysts, *Zaduzbina Andrejevic, Beograd*.
22. Zhang, F.; Zhao, J.; Zang, L.; Shen, T.; Hidaka, H., Pelizzetti, E.; Serpone, N. (1997) Photoassisted degradation of dye pollutants in aqueous TiO<sub>2</sub> dispersions under irradiation by visible light, *J. Mol. Catal. A-Chem.* 120 [1–3], 173–178. [http://dx.doi.org/10.1016/S1381-1169\(96\)00405-0](http://dx.doi.org/10.1016/S1381-1169(96)00405-0).
23. Hadnadjev-Kostic, M.; Vulic, T.; Ranogajec, J.; Marinkovic-Neducin, R.; Radosavlajevic-Mihajlovic, A. (2013) Thermal and photocatalytic behavior of TiO<sub>2</sub>/LDH nanocomposites, *J. Term. Anal. Calorim.* 111 [2], 1155–1162. <http://dx.doi.org/10.1007/s10973-012-2226-5>.
24. Saravanan, R.; Thirumal, E.; Gupta, V.K.; Narayanan, N.; Stephen, A. (2013) The photocatalytic activity of ZnO prepared by simple thermal decomposition method at various temperatures *J. Mol. Liq.* 177, 294–401. <http://dx.doi.org/10.1016/j.molliq.2012.10.018>.
25. Vulić, T.; Hadnadev-Kostić, M.; Marinković-Nedućin, R.; Ranogajec, J. (2011) Study of Novel Mesoporous Photocatalysts Based on TiO<sub>2</sub>/Zn–Al Layered Double Hydroxides, Heron press Ltd. Eds. K. Hadjiivanov, V.Valtchev, S. Mintova, G. Vayssilov, *Topics in Chemistry and Material Science*, 6, 2011, pp. 182–192. ISSN 1314-0795.
26. Chong, M.N.; Vimonses, V.; Lei, S.; Jin, B.; Chow, C.; Saint, C. (2009) Synthesis and characterization of novel titania impregnated caolinite nano-photocatalyst. *Micropor. Mesopor. Mat.* 117, 233–242. <http://dx.doi.org/10.1016/j.micromeso.2008.06.039>.
27. Reli, M.; Koci, K.; Matějka, V.; Kovár, P.; Obalová, L. (2012) Effect of calcination temperature and calcination time on the kaolinite/TiO<sub>2</sub> composite for photocatalytic reduction of CO<sub>2</sub>. *Geo Science Engineering* LVIII [4], 10–22.